Ground penetrating radar characterization of fault-generated Quaternary colluvio-fluvial deposits along the seismically active Kachchh Mainland Fault, Western India

V. Chowksey, P. Joshi, D. M. Maurya* and L. S. Chamyal

Department of Geology, The M.S. University of Baroda, Vadodara 390 002, India

Quaternary colluvio-fluvial deposits in the seismically active Kachchh Mainland Fault (KMF) zone have been studied using ground penetrating radar (GPR). The deposits form a north-sloping ~2–3 km wide, deeply dissected surface to the north of the KMF scarps developed in Mesozoic rocks forming the northern limb of the Habo dome. The northward slope of the surface and decreasing trend of incision towards the north are attributed to neotectonic activity along KMF. Exposed river sections and trench sections correlate well with the GPR data. The various sedimentary facies identified vary from bouldery gravel to finer gravel and gravelly sand. Discontinuous wavy radar reflections relate to bouldery gravel deposits, whereas the parallel discontinuous reflections indicate finer gravels or gravelly sands. In contrast, the parallel and continuous radar reflections characterize the well-stratified gravels. The study demonstrates the utility of GPR in colluvial and reworked colluvial deposits in active fault zones.

Keywords: Colluvio-fluvial deposits, ground penetrating radar, neotectonic activity, sedimentary facies.

THE Kachchh Mainland Fault (KMF) is a major intrabasinal fault of the Kachchh basin (Figure 1 *a*). The fault is known to be seismically active as evidenced by several earthquakes, including the *Mw* 7.7 earthquake in 2001 (ref. 1). Geomorphologically, the fault is expressed as a linear series of north-facing E–W trending scarps. However, neotectonic characterization and detailed mapping of Quaternary deposits along KMF have not been done. In this communication we describe the results of ground penetrating radar (GPR) studies on the colluvio-fluvial deposits in a part of the KMF zone. The present study is based on field mapping and GPR studies of the Quaternary colluvio-fluvial deposits associated with KMF. The area of the study includes the colluvio-fluvial surface located to the north of the Habo dome (Figure 1 *b*). The colluvio-fluvial deposits exposed along the incised cliffs of various north-flowing streams were studied. Vertical lithologs were prepared at several locations. The sedimentological characteristics, particularly the downstream variation in the nature of sediments were documented. GPR surveys were carried out at selected sites to understand geophysical signatures of the various sedimentary facies associated with the colluvio-fluvial deposits occurring in the KMF zone (Figure 2 *a*).

The Habo dome is one of the largest domal structures developed along E–W trending faults in Kachchh[2]. The overall topography over the Habo dome is rugged and highly dissected (Figure 1 *b*). The dome exposes Mesozoic rocks, with intrusive rocks in the core portion of the dome[3]. The dome is confined to the east by the Kaswali River and to the west by the Khari River (Figure 2 *a*). Both rivers flow along courses that are controlled by the transverse faults[4]. KMF has significantly controlled the structural and physiographic set-up of this part of the terrain. On account of this fault, the northern limb of the dome is steeper, whereas the southern limb coinciding with the southward dip of the strata is gentler[2]. The rugged, mountainous terrain of the Habo dome suggests neotectonic rejuvenation along KMF to the north[5].

The drainage displays a strong control of the structural set-up. The drainage pattern developed over the Habo dome is radial, which is in conformity with the structure (Figure 2 *a*). The drainage density is high, with several small and large streams flowing outward in a radial movement from the centre of the dome. The various rivers show deep valleys that are incised into the Mesozoic rocks with occasional development of gorges. The streams flowing towards east and south meet the Kaswali River, whereas those flowing westward meet the Khari River (Figure 2 *a*). The Khari River arises from the Katrol Hills in the central mainland and flows northward to meet the Banni Plain. The Kaswali River arises from the Habo hills and flows north towards Lodai, and finally merges in the Banni Plain by splitting into several shallow, sandy distributary channels. The northward-flowing streams are however significant as they cut across the KMF scarps and follow incised valleys before disappearing into the Banni Plain (Figure 2 *a*). The Quaternary deposits within the rugged terrain of Habo dome are extremely patchy. However, the north-flowing streams after crossing the KMF scarps incise through the Quaternary deposits. The streams are characterized by the straight channel courses, incised banks in alluvial and rocky terrains, anomalous widening and narrowing of channels and valleys, high-angle deflected channels and development of entrenched meanders that typically point to the role of active tectonism in the landscape evolution.

The E–W trending line of north-facing scarps forms a prominent geomorphic expression of KMF. The scarps are developed in the Mesozoic rocks forming the steeply dipping northern limb of the Habo dome (Figure 1 *b*). However, the scarps do not mark the fault line of KMF as the Mesozoic rocks are found to continue further north and consequently, the main fault is presumed to be

*For correspondence. (e-mail: dmmaurya@yahoo.com)

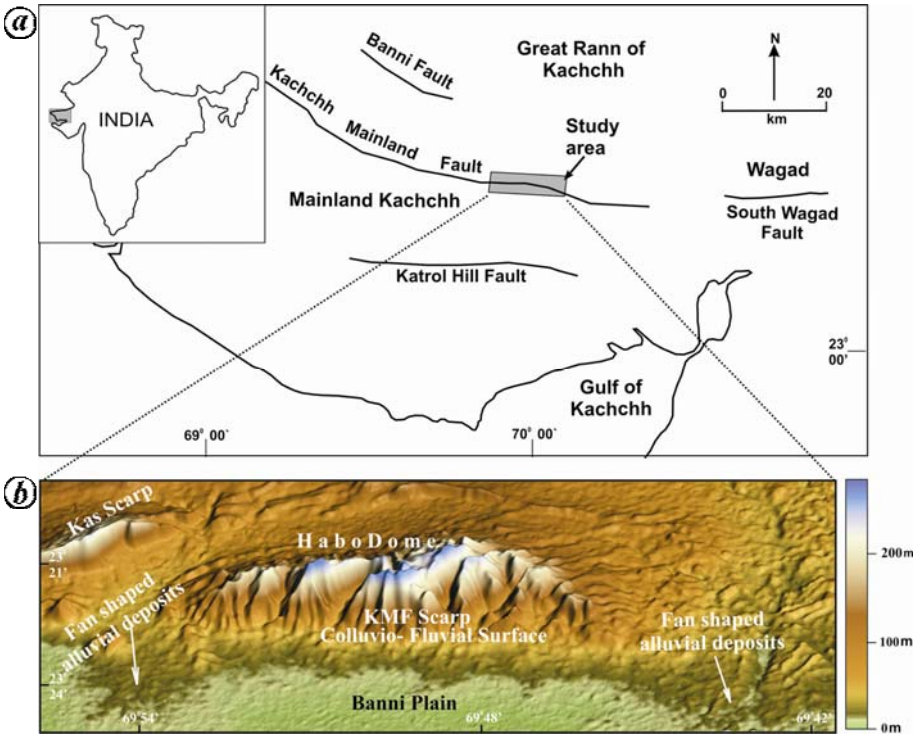

Figure 1. ***a***, Map of Kachchh showing the major faults and the area of the present study. (Inset, Location map.) ***b***, Digital elevation model providing a south-facing view of the study area prepared from ASTER data highlighting the geomorphic set-up of the Kachchh Mainland Fault (KMF) zone.

buried under the cover of Quaternary sediments lying in front of the scarps. The scarps are therefore retreated scarps. The scarp line is broken by several streams which cut through them and northward towards the Banni Plain. The scarps show sub-vertical to vertical faces indicating neotectonic rejuvenation due to movements along KMF. Overall, the KMF scarps exhibit characteristics typical of an active mountain front.

The colluvio-fluvial surface is a distinct geomorphic surface developed over the Quaternary sediments to the north of the scarps (Figures 1 *b* and 2 *a*, *b*). The surface is characterized by a distinct northward slope and is confined between the scarp line and the Banni Plain (Figure 2 *a*). The boundary between this Quaternary surface and the Banni Plain is transitional and is marked by a thin strip of alluvium. The digital elevation model of the area clearly bring out this northward-sloping surface, which is distinctly identifiable from a flat, gradientless Banni Plain (Figure 1 *b*). The pronounced northward slope of this surface made of Quaternary colluvio-fluvial deposits suggests neotectonic reactivation of KMF. The surface is highly dissected, exposing the sediments along the 2–10 m incised cliffs on the various north-flowing streams (Figure 2 *c*). The progressive decrease in the depth of fluvial incision towards north to < 1 m as the streams approach the Banni Plain, substantiates the tectonic tilting of the surface due to neotectonic activity along KMF.

Fan-shaped sandy alluvium deposited by the Khari and Kaswali rivers at the intersection of the northern hill range with the Banni Plain is another conspicuous feature of the KMF zone (Figure 2 *a*). The fan shape of the deposits is primarily formed by offloading of sandy sediments by these rivers as they come out of the northern hill range and break up into small distributary channels as they can flow no further. The Banni Plain, considered as a part of the Great Rann, is a flat and almost gradientless saline grassland. The geological evolution of the Banni Plain is related to marine processes during the Holocene[6]. In general, the plain of Banni is regarded as a raised mudflat between the Mainland Kachchh and the salt encrusted surface of the Great Rann[6].

The Quaternary deposits have extensively developed along a 2–3 km wide narrow strip to the north of the KMF scarps. These sediments are mostly colluvio-fluvial deposits and are significant indicators of neotectonic rejuvenation of KMF. The deposits form a distinct geomorphic surface that abuts against the KMF scarps in the south (Figure 2 *b*). Towards north the surface shows a transitional to abrupt contact with the flat surface of the Banni Plain. As mentioned earlier, the colluvio-fluvial surface shows a gentle slope towards north. Near the scarps the surface shows an elevation of ~ 40 m and merges with the Banni Plain surface, which is about 4–6 m amsl. The colluvio-fluvial surface is dissected by several lower-order streams that arise from the KMF scarp line (Figure 2 *b* and *c*). The streams flow towards north, incising through these deposits, thereby exposing the colluvio-fluvial deposits along the cliff sections

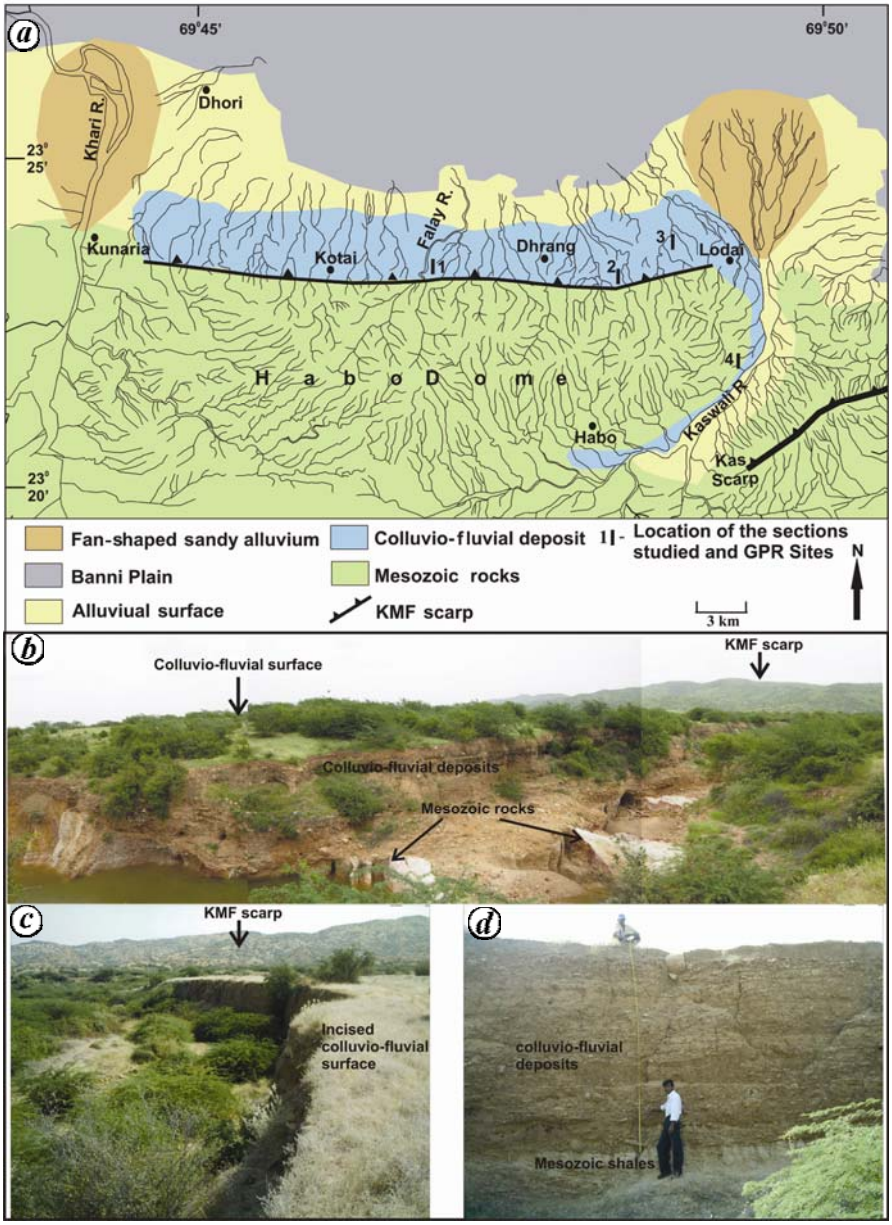

Figure 2. ***a***, Geomorphological map of the study area showing major geomorphic units. Locations of the sections studied and ground penetrating radar (GPR) sites are also shown. ***b***, Panoramic view of the KMF zone showing the field setting of the Quaternary colluvio-fluvial deposits along the Falay River. Note the flat surface in the front of the KMF scarps formed over the colluvio-fluvial deposits exposed along the incised cliffs of the river. Also seen are the vertical to sub-vertical highly sheared Mesozoic rocks marking KMF and the sharp unconformable contact with the overlying stratified colluvio-fluvial deposits. GPR survey (site 1) was carried out at the left-hand corner of the photograph. ***c***, View of the incision of colluvio-fluvial surface by a stream to the east of Dhrang. ***d***, View of the exposed section in the incised cliff shown in (***b***). Note the Mesozoic shales at the base and the distinct depositional phases. Height of the person is 170 cm.

(Figure 2 *c*). The depth of incision is found to be maximum (~ 10 m) near the scarps, which rapidly decreases towards north. The decrease in the depth of incision is consistent with the northward gradient of the surface.

The deposits are of coarse nature and are exposed in incised cliff sections along the north-flowing streams (Figure 2 *b* and *c*). Closer to the scarps the deposits are found to overlie the steeply dipping and at places sheared Mesozoic rocks (Figure 2 *b*). The eroded surface of the Mesozoic rocks marks a distinct unconformity over which the colluvio-fluvial sediments were deposited. The colluvio-fluvial deposits indicate deposition in well-marked phases and are at places well stratified (Figure 2 *d*). Overall, the deposits comprise horizontal to subhorizontal layers of gravelly to pebbly colluvio-fluvial material with elongated lensoid bodies of sand. The coarser layers, mostly matrix-supported gravels and pebbles, are devoid of internal stratification. In some sections, large

clasts comprising subrounded cobbles and boulders form distinct bouldery gravel beds, and they may also be randomly distributed within finer gravels. The size of the large clasts may vary from 0.5 to more than 1 m. The fact that these deposits occur only in the narrow area between the north-facing scarps marking KMF and the flat terrain of the Banni Plain is a significant indicator of the neotectonic reactivation of KMF (Figure 2 *a*).

GPR is a noninvasive geophysical technique that detects electrical discontinuities in the shallow subsurface (< 50 m) using electromagnetic (EM) waves typically in the 1–1000 MHz frequency. It involves transmission of high frequency EM pulse of energy into the ground, which radiates downward and at sediment interfaces some of the energy is reflected back to the surface[7]. The basic principles of seismic data processing and interpretation are used in GPR data interpretation[8]. GPR is now increasingly applied in shallow subsurface studies and sediment characterization in active fault zones for delineating neotectonic and palaeoseismic activities[9–14]. However, of particular relevance to the present study, are the recent studies that demonstrate successful application of GPR in the characterization of colluvial and other coarse-grained deposits of diverse origins in varied geomorphic settings[15–21]. Based on radar reflections, the subsurface lithological characteristics of different types of coarse-grained deposits and depth of basement rocks have been delineated[15–21].

We carried out 2D GPR surveys with a GSSI SIR-20 system using a 200 MHz antenna along N–S oriented transects at four sites for studying the colluvio-fluvial deposits (Figure 2 *a*). The lithologs of the exposed colluvio-fluvial sediments at these sites are shown in Figure 3. The N–S transects were preferred to allow for correlation with the exposed cliff sections. Several trial profiles were obtained to determine appropriate acquisition parameters to get the final GPR profiles. A time window of 100–125 ns with a sampling rate of 512 samples/scan was found adequate. Three common midpoint (CMP) profiles were collected from the area and a velocity of 0.124 m/ns was found adequate for the time–depth conversion. Post-survey processing of GPR data was done using the RADAN software. The processing steps applied include simple trace-editing, band-pass filtering, static correction, stacking and amplification of weak signals using gain function. All profiles shown here are time-zero corrected and presented in wiggle trace format.

Identifying radar facies is an important criterion for geophysical characterization of sedimentary deposits[22]. Radar facies are generally characterized on the basis of shape, amplitude, continuity and internal configuration[22–25]. Each radar facies is different from the adjacent group of reflectors and is interpreted in terms of the sedimentary characteristics, preferably by correlation of radar wave behaviour with exposed sediments[15]. The GPR data generated during the present study were interpreted in conjunction with the exposed sediment in cliff sections. A description of the GPR study and its interpretation at various sites is given below.

Site 1 is located north of the scarps along the Falay River that arises from the central part of the Habo dome and flows northward incising through Quaternary colluvio-fluvial deposits (Figure 2 *a*). At this site, the deposits unconformably overlie the highly sheared Mesozoic rocks showing vertical dips which mark the KMF zone (Figure 4 *a*). The exposed section shows ~4.5 m of crudely stratified colluvio-fluvial deposits with the basal part of the section consisting of sheared Mesozoic rocks. The GPR survey was carried out on top of the cliff section using 200 MHz antenna along the N–S transect. The processed profile is shown in Figure 4 *a*. The profile depicts three major radar facies – the upper part comprising discontinuous inclined reflectors, followed by continuous and parallel high-amplitude reflectors, and low-amplitude parallel discontinuous reflectors. The lower part shows high attenuation of radar energy due to the fine-grained and sheared lithologies of the Mesozoic rocks. The inclined reflectors observed in the upper part are usually produced by cross-bedded strata[17,21]. However, here it is due to the coarse pebbly–cobbly deposits that were laid down on a scoured erosional palaeo-surface. The colluvio-fluvial layers in the deposits attained low dips in conformity with the unevenness of the available surface. The underlying parallel continuous reflectors were produced by the crude horizontal stratification of the colluvio-fluvial deposits[17]. The reflectors appear to have been formed due to the clast-rich layers alternating with relatively clast-poor

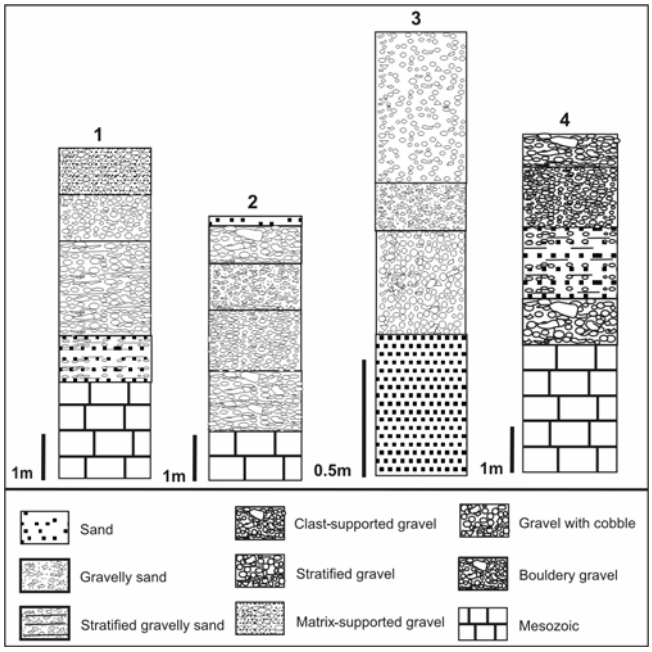

Figure 3. Lithologs of exposed sections of Quaternary colluvio-fluvial deposits at sites 1–4. Sites 1, 2 and 4 are of river cliff sections, whereas site 3 is from a pit section. Location of lithologs is shown in Figure 2 *a*.

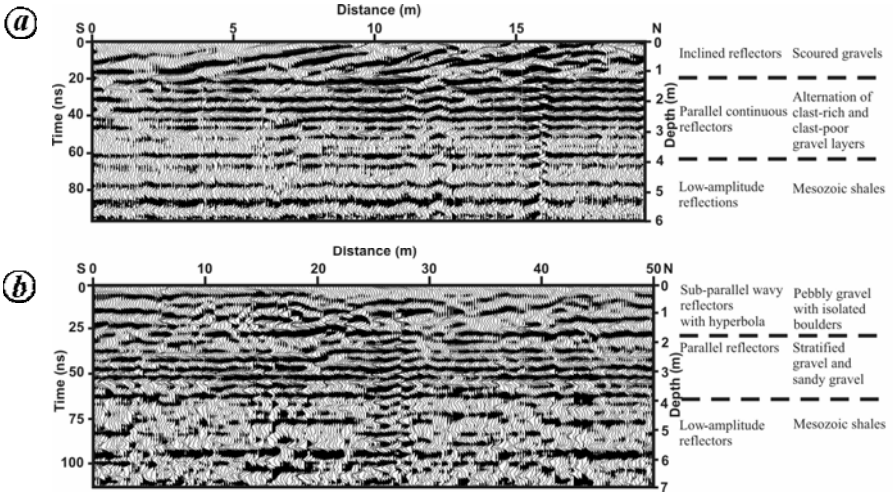

Figure 4. The 200 MHz monostatic antenna GPR profiles in wiggle mode. Various radar facies and corresponding lithologies are indicated against each profile. Location of sites is shown in Figure 2 *a*. ***a***, S–N profile from site 1 near Falay River showing three distinct radar facies. ***b***, S–N profile from site 2 showing three distinct radar facies.

layers. The low-amplitude parallel discontinuous reflections are attributed to the presence of sand with finer gravel[17].

Site 2 is located between the scarp line and the KMF zone that lies further north (Figure 2 *a*). The incised cliff section here is about 6 m high, that exposes 4 m of Quaternary colluvio-fluvial deposits unconformably overlying the Mesozoic shales. The colluvio-fluvial deposits consist of well-stratified gravels and sandy gravel layers. The gravels are mostly of pebble size; however, some of the layers contain isolated boulder-size clasts of Mesozoic sandstones. The GPR data were obtained by moving the 200 MHz antenna along the N–S transects on top of the cliff section. The GPR profile (Figure 4 *b*) shows data up to the depth of 7 m. The GPR profile is divisible into two distinct parts. In the lower part of the profile up to 4.5 m depth, low-amplitude signals with reflections not showing any particular pattern are observed. Attenuation of the radar signal is generally observed in the clay-rich sediments[21]. Here it is on account of the northward-dipping Mesozoic shale. The upper part of profile corresponding to the colluvio-fluvial deposits shows three major radar facies. The upper part of the profile up to 1.5 m shows subparallel to wavy reflections with distinct hyperbolas. The reflections correspond to the matrix-poor pebbly gravels with an erosional base[16,17]. The hyperbolas are on account of isolated, subrounded to angular boulders of Mesozoic sandstone. Below this, a zone of (1.5–3.5 m depth) high-amplitude parallel reflectors is observed. These correlate with the alternate layers of horizontally stratified gravel and sandy gravel[19]. The contacts of these layers are sharp resulting in distinct parallel reflections. Small hyperbolas within this zone are attributed to the floating boulder-size clasts in the gravel layers.

Site 3 is located to the west of Lodai (Figure 2 *a*). The GPR survey was carried out above a pit section dug by local people. The pit was 2 m deep and the section exposed in the pit wall was 14 m long. Since the site is the farthest from the scarp line compared to other sites, the colluvio-fluvial deposits here were found to be of finer gravel. The 200 MHz antenna was dragged over the pit wall and the data obtained were compared with the exposed section. The GPR radar profile (Figure 5 *a*) shows good correlation with the exposed pit section. The entire profile shows two distinct types of reflection. The upper part up to 3.5 m depth exhibits high-amplitude returns interpreted as the total thickness of colluvio-fluvial deposits at the site. In this part, three major radar facies are identified, which comprise of high-amplitude discontinuous parallel reflectors, relatively low-amplitude discontinuous parallel reflectors and high-amplitude continuous parallel reflectors. The parallel, discontinuous, high-amplitude reflections correspond to the matrix-supported stratified gravels that form the top part of the exposed pit section. The high-amplitude, parallel, continuous radar facies is found to grade laterally into discontinuous parallel reflections of low amplitude. Comparison of GPR data with the exposed section in the pit indicates that the grading of the radar facies is closely related to the lateral variation of the clast-rich gravel into matrix-rich gravel. Thickening and thinning of the individual strata are also observed in the exposed section. In general, high-amplitude, parallel, continuous radar facies is found to have been produced by the clast-rich gravels (less matrix), whereas the discontinuous, parallel reflections of low-amplitude are attributable to gravels with more matrix[17]. Collectively, the three radar facies suggest that the thickness of colluvio-fluvial deposits at the site is about 3.5 m, of which, the upper 2 m is exposed in the pit section. Reflections below 3.5 m depth are found to be of low amplitude and highly attenuated which is interpreted as fine-grained lithology, possibly shales forming the

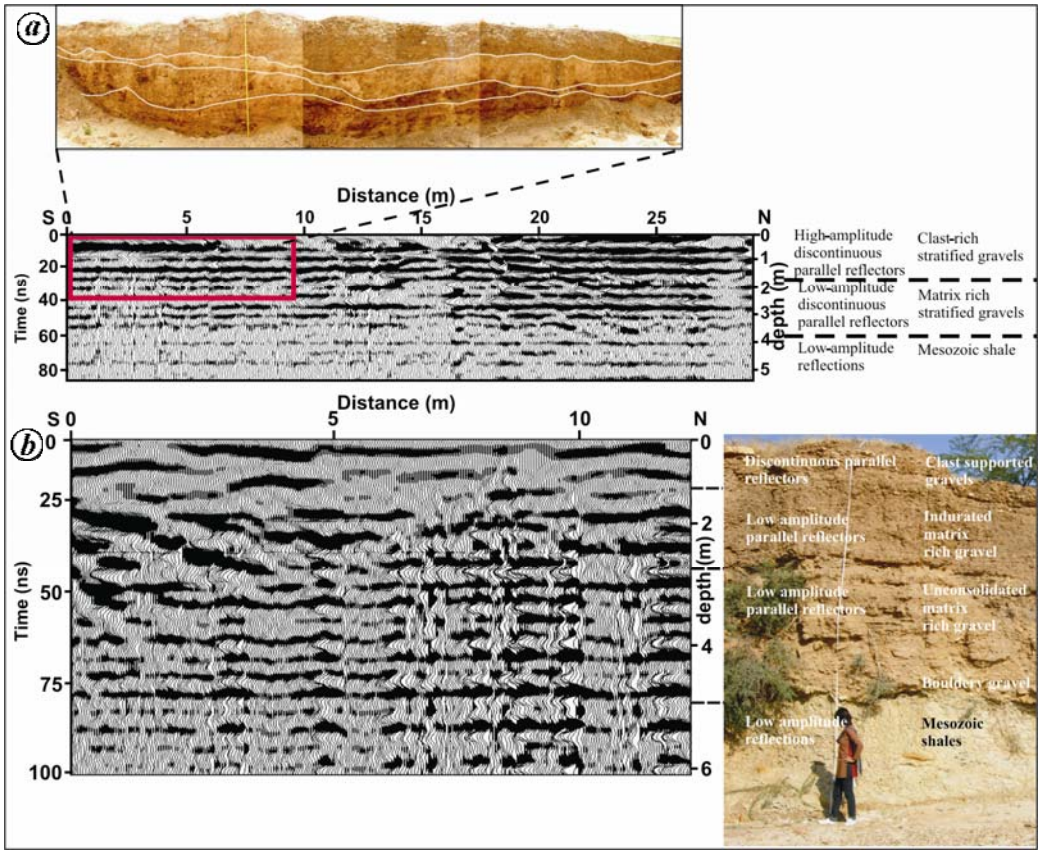

Figure 5. The 200 MHz monostatic antenna GPR profiles in wiggle mode. Various radar facies and corresponding lithologies are indicated against each profile. Location of sites is shown in Figure 2 *a*. ***a***, S–N profile from site 3. Photograph shows the exposed pit section. The rectangular box in the profile corresponds to the exposed pit section. ***b***, S–N profile from site 4 with photograph of the river section. Height of the person is 1.58 m.

basement of the colluvio-fluvial deposits. This is further supported by the fact that the Mesozoic rocks are exposed on the surface very close to the south and east of the site.

Site 4 is located behind (south) the scarp line along the left bank of the Kaswali River at the eastern fringe of the Habo dome (Figure 2 *a*). The studied section is located along the incised cliff section of the Kaswali River. Here, the 6.5 m section exhibits colluvio-fluvial deposits underlain by Mesozoic rocks (Figure 5 *b*). The GPR data were obtained by dragging the 200 MHz antenna on top of the cliff section. As seen at other sites, the GPR data (Figure 5 *b*) for this site are also characterized by attenuation of radar waves below 4.5 m, which is attributable to the Mesozoic rocks forming the base of the exposed section. However, attenuation is of less magnitude compared to the other sites mainly because the Mesozoic rocks here consist of alternations of thinly bedded sandstone and shale. The overlying group of reflectors (1.5–4.5 m) comprises parallel and consistent reflections. In the exposed section, the corresponding lithology consists of the basal bouldery gravel (1 m thick), followed by unconsolidated matrix-rich gravel (1.5 m thick) and indurated matrix-rich gravel (1.5 m thick). The lithology of the later two horizons is similar, though both are readily distinguished in the section owing to the variation in the degree of induration. However, both are represented by the same radar facies because of the similarity in gross lithology. The basal bouldery horizon is also not clearly picked in the profile, which could be due to the laterally discontinuous and dispersed nature of the boulders. Also, we cannot rule out the possibility of the absence of boulders at this depth along the profile line which was about 1.5 m away from the vertical cliff face. The uppermost part of the profile shows reflections marked by several partial and incomplete hyperbola formations and few inclined reflectors as well. These correlate with the uppermost horizon consisting of clast-supported gravel with randomly distributed cobbles, possibly, responsible for the indistinct hyperbolas[18].

The field and GPR based study carried out on the colluvio-fluvial deposits has proved useful for understanding the geomorphological and neotectonic setting of the E–W trending KMF zone. The fault is morphologically expressed as E–W trending steep scarps, while the actual fault line is located further north and is buried under the Quaternary colluvio-fluvial sediments. The northward-tilted apron of colluvio-fluvial deposits overlapping the fault zone and incised fluvial valleys point to the neotectonically active nature of the KMF. The exposed sections studied reveal vertical and lateral variation of the

colluvio-fluvial sediments. The sedimentary facies observed comprise bouldery layers, semi-compacted to compacted clast-rich to matrix-rich gravels, and sandy gravels. In general, it was found that the radar facies correlated well with the sedimentary facies seen in the exposed sections. Three major radar facies have been identified, which are easily distinguished from the adjacent radar reflections. The discontinuous inclined to wavy reflections with indistinct hyperbolas relate to coarse gravel deposits with floating boulders. The discontinuous, wavy reflections are produced by the interfaces between the cross-bedded, fine, sandy layers and gravel layers[25]. Formation of hyperbolas is attributed due to scattering radar waves from large clasts (> 30 cm)[15]. The second radar facies comprising parallel discontinuous reflections is found to be produced by sandy gravel or matrix-rich gravel[17]. Well-stratified gravel was found responsible for the third radar facies consisting of parallel and continuous radar reflections. The basement rocks comprising Mesozoic shales were clearly visible in the GPR data as a zone of attenuation of radar waves below the high-amplitude reflections representing the colluvio-fluvial deposits. In such cases, the bedrock interface may not necessarily produce a strong reflector, instead fading of radar signals can be observed corresponding to basement rocks consisting of fine-grained and sheared lithologies[18]. The present study shows that GPR is a potential tool for mapping and understanding subsurface nature of the colluvio-fluvial sediments occurring in the KMF zone. Moreover, GPR studies using antennas of lower frequencies may be used for precise mapping of the KMF fault line which is buried under these sediments. The observations made in the present study warrant similar studies along the entire length of KMF.

1. Biswas, S. K. and Khattri, K. N., A geological study of earthquakes in Kachchh, Gujarat, India. *J. Geol. Soc. India*, 2002, **60**, 131–142.
2. Biswas, S. K., Regional tectonic framework structure and evolution of the western margin basin of India. *Tectonophysics*, 1987, **135**, 307–327.
3. Biswas, S. K., *Geology of Kutch*, K.D. Malaviya Institute of Petroleum Exploration, Dehradun, 1993, p. 450.
4. Maurya, D. M., Thakkar, M. G. and Chamyal, L. S., Implication of transverse fault system on tectonic evolution of Mainland Kachchh, western India. *Curr. Sci.*, 2003, **85**, 661–667.
5. Thakkar, M. G., Maurya, D. M., Raj, R. and Chamyal, L. S., Quaternary tectonic history and terrain evolution of the area around Bhuj, mainland Kachchh, western India. *J. Geol. Soc. India*, 1999, **53**, 601–610.
6. Kar, A., Geomorphology of the western India. *Mem. Geol. Soc. India*, 1995, 32, 168–190.
7. Neal, A., Ground-penetrating radar and its use in sedimentology: principles, problems and progress. *Earth Sci. Rev.*, 2004, **66**, 161–330.
8. Davis, J. L. and Annan, A. P., Ground-penetrating radar for high-resolution mapping of soil and rock stratigraphy. *Geophys. Prospect.*, 1989, **37**, 531–551.
9. Patidar, A. K., Maurya, D. M., Thakkar, M. G. and Chamyal, L. S., Fluvial geomorphology and neotectonic activity based on field and GPR data, Katrol hill range, Kachchh, western India. *Quaternary Int.*, 2007, **159**, 74–92.
10. Patidar, A. K., Maurya, D. M., Thakkar, M. G. and Chamyal, L. S., Evidence of neotectonic reactivation of the Katrol Hill Fault during late Quaternary and its GPR characterization. *Curr. Sci.*, 2008, **94**, 338–346.
11. Smith, D. G. and Jol, H. M., Wasatch fault (Utah), detected and displacement characterized by ground-penetrating radar. *Environ. Eng. Geosci.*, 1995, **1**, 489–496.
12. Chow, J., Angelier, J., Hua, J.-J., Lee, J.-C. and Sun, R., Paleoseismic event and active faulting from ground penetrating radar and high resolution seismic reflection profiles across the Chihshang fault, eastern Taiwan. *Tectonophysics*, 2001, **333**, 241–259.
13. Christie, M., Tsoflias, G. P., Stockli, D. F. and Black, R., Assessing fault displacement and of-fault deformation in an extensional tectonic setting using 3-D ground penetrating radar imaging. *J. Appl. Geophys.*, 2009, **68**, 9–16.
14. Stepancikova, P., Hok, J., Nyvlt, D., Dohnal, J., Sykorova, I. and Stemberk, J., Active tectonics research using trenching technique on the south-eastern section of the Sudetic Marginal Fault (NE Bohemian Massif, central Europe). *Tectonophysics*, 2010, **485**, 269–282.
15. Sass, O. and Krautblatter, M., Debris flow-dominated and rockfall-dominated talus slopes: Genetic models derived from GPR measurements. *Geomorphology*, 2007, **86**, 176–192.
16. Fiore, J., Pugin, A. and Beres, M., Sedimentological and GPR studies of subglacial deposits in the Joux Valley (Vaud, Switzerland): backset accretion in an esker followed by an erosive jökulhlaup. *Géogra. Phys. Quat.*, 2002, **56**, 19–32.
17. Kostic, B. and Aigner, T., Sedimentary architecture and 3D ground-penetrating radar analysis of gravelly meandering river deposits (Neckar Valley, SW Germany). *Sedimentology*, 2007, **54**, 789–808.
18. Sass, J., Bedrock detection and talus thickness assessment in the European Alps using geophysical methods. *J. Appl. Geophys.*, 2007, **62**, 254–269.
19. Beres, M., Huggenberger, P., Green, A. G. and Horstmeyer, H., Using two and three-dimensional georadar methods to characterize glaciofluvial architecture. *Sediment. Geol.*, 1999, **129**, 1–24.
20. Ekes, C. and Hickin, E. J., Ground penetrating radar facies of the paraglacial Cheekye Fan, southwestern British Columbia, Canada. *Sediment. Geol.*, 2001, **143**, 199–217.
21. Overmeeren, R. A. V., Radar facies of unconsolidated sediments in The Netherlands: a radar stratigraphy interpretation method for hydrogeology. *J. Appl. Geophys.*, 1998, **40**, 1–18.
22. Jol, H. M. and Bristow, C. S., GPR in sediments: advice on data collection, basic processing and interpretation, a good practice guide. In *GPR in Sediments* (eds Bristow, C. S. and Jol, H. M.), Spec. Publ.–Geol. Soc. Lond., 2003, vol. 211, pp. 9–27.
23. Cassidy, N. J., Ground penetrating radar theory and application. In *Ground Penetrating Radar: Processing, Modeling and Analysis* (ed. Jol, H. M.), Elsevier, 2009, pp. 141–172.
24. Woolridge, C. L. and Hickin, E. J., Radar architecture and evolution of channel bars in wandering gravel-bed rivers: Fraser and Squamish rivers, British Columbia, Canada. *J. Sediment. Res.*, 2005, **75**, 844–860.
25. Kostic, B., Becht, A. and Aigner, T., 3-D sedimentary architecture of a Quaternary gravel delta (SW-Germany): Implications for hydrostratigraphy. *Sediment. Geol.*, 2005, **181**, 143–171.

ACKNOWLEDGEMENTS. We thank the Department of Science and Technology and Ministry of Earth Sciences, Government of India for providing funds. Constructive reviews by the two anonymous reviewers helped improve the manuscript.

Received 1 July 2010; revised accepted 3 February 2011